Nonsimilar solutions for free convection from a nonisothermal vertical plate in a micropolar fluid

Received November 1996
Revised February 1997

I.A.Hassanien
Department of Mathematics, Assuit University, Assuit, Egypt, and
Rama Subba Reddy Gorla
Department of Mechanical Engineering, Cleveland State University, Cleveland, Ohio, USA

Nomenclature

g	=	dimensionless microrotation component
g	=	acceleration due to gravity
h	=	heat transfer coefficient
j	=	microinertia per unit mass
k	=	thermal conductivity of the fluid
N	=	angular velocity
Nu	=	Nusselt number
Pr	=	Prantl number
q_w	=	surface heat flux
Re	=	Reynolds number
T	=	temperature
u	=	velocity in *x*-direction
v	=	velocity in *y*-direction
x,y	=	co=ordinate parallel and normal to the plate
β	=	coefficient of thermal expansion
γ	=	micropolar material property
ξ, η	=	dimensionless coordinates
Δ. λ, B	=	dimensionless material parameters
θ	=	dimensionless temperature
κ	=	microrotation viscosity parameter
μ	=	viscosity
ν	=	kinematic viscosity
ρ	=	density of fluid

Subscripts

w	=	surface condition
∞	=	condition far away from the surface

Introduction

The classical Navier-Stokes theory does not adequately describe the flow properties of polymeric fluids and some naturally occurring fluids such as animal blood. The theory of micropolar fluids, first proposed by Eringen[1] is capable of describing such fluids. In this theory, the local effects arising from the microstructure and the intrinsic motion of the fluid elements are taken into account.

Micropolar fluids consist of a suspension of small, rigid, cylindrical elements such as large dumbbell-shaped molecules. Micropolar fluids are non-Newtonian fluids with microstructures such as polymeric additives, colloidal suspensions, animal blood, liquid crystals etc. Eringen[2] extended the theory of micropolar fluids to describe the theory of thermomicropolar fluids.

The authors are grateful to the reviewers for their helpful advice.

Ahmadi[3] derived a similarity solution for the boundary layer flow of a micropolar fluid over a flat plate. The forced convective heat transfer in the micropolar boundary layer flow along a horizontal plate was studied by Gorla[4]. Jena and Mathur[5] presented a similarity solution for the free convection in micropolar fluids along a vertical plate. Recently, Gorla[6-8] investigated the mixed convection in micropolar boundary layer flow along vertical and horizontal plates. Gorla[6,7] presented asymptotic boundary layer solutions for the combined convection from a vertical plate to a micropolar fluid. The boundary conditions of uniform surface temperature and heat flux were considered. Consideration was given to the region close to the leading edge as well as the region far away from the leading edge. Numerical results were obtained for the velocity, angular velocity and temperature fields. The effects of buoyancy-induced streamwise pressure gradients on laminar forced convection heat transfer to micropolar fluids from a horizontal plate were investigated by Gorla[8]. He presented numerical solutions for the transformed boundary layer equations for different values of the buoyancy and material parameters.

This work is concerned with the nonsimilar free convection in micropolar fluids along a nonisothermal vertical plate. The nonsimilarity arises due to the nonuniform nature of the surface temperature distribution. Three specific forms are assumed for the surface temperature distribution. For these cases, the nonsimilar conservation laws are derived and numerical solutions are obtained for the details of the velocity, microrotation and temperature fields as well as friction factor and Nusselt number variations.

Analysis

Consider the steady natural convection flow from a heated vertical plate placed in a micropolar fluid. Let the co-ordinates be chosen such that *x* measures the distance from the leading edge of the plate and *y* measures the distance normal to the plate. The temperature of the quiescent ambient fluid at large values of y is taken to be constant at T_∞.

The equations governing the conservation of mass, momentum, angular momentum and energy can be written in a dimensionless form as:

Mass

$$\frac{\partial \bar{u}}{\partial \bar{x}} + \frac{\partial \bar{v}}{\partial \bar{y}} = 0 \tag{1}$$

Momentum

$$\bar{u}\frac{\partial \bar{u}}{\partial \bar{x}} + \bar{v}\frac{\partial \bar{u}}{\partial \bar{y}} = (1+\Delta)\frac{\partial^2 \bar{u}}{\partial \bar{y}^2} + S_w(\bar{x})\theta + \Delta\frac{\partial \bar{N}}{\partial \bar{y}} \tag{2}$$

Moment of momentum

$$\bar{u}\frac{\partial\bar{N}}{\partial\bar{x}}+\bar{v}\frac{\partial\bar{N}}{\partial\bar{y}}=-B\Delta(2\bar{N}+\frac{\partial\bar{u}}{\partial\bar{y}})+\lambda\frac{\partial^2\bar{N}}{\partial\bar{y}^2} \quad (3)$$

Energy

$$\bar{u}\left[\frac{\partial\theta}{\partial\bar{x}}+\theta\frac{d\ln S_w(\bar{x})}{d\bar{x}}\right]+\bar{v}\frac{\partial\theta}{\partial\bar{y}}=\frac{1}{Pr}\frac{\partial^2\theta}{\partial\bar{y}^2} \quad (4)$$

The boundary conditions may be written as

$$\bar{y}=0 \quad \bar{u}=\bar{v}=0, \qquad \bar{N}=0 \quad \theta=1$$
$$\bar{y}\to\infty, \qquad \bar{u}=\bar{N}=\theta=0 \quad (5)$$

Equations (1-5) appear in dimensionless form based on the following relations:

$$\bar{x}=x/L, \bar{y}=y\sqrt{Re}/L, \bar{u}=u/u_c, \bar{v}=v\sqrt{Re}/u_c$$
$$\bar{N}=\nu\sqrt{Re}N/u_c^2, \theta=\frac{T(x,y)-T_\infty}{T(x,0)-T_\infty}, u_c=\sqrt{g\beta(T_r-T_\infty)L}, Re=u_cL/\nu$$
$$\Delta=\kappa/\mu, \lambda=\gamma/\mu j, B=\mu L/\rho j u_c, S_w(\bar{x})=\frac{T(x,0)-T_\infty}{T_r-T_\infty} \quad (6)$$

where u and v are the velocity components in x and y directions, ρ is the density, μ is the viscosity, j is the micro-inertia density per unit mass, β is the coefficient of expansion, ν is kinematic viscosity, N is the component of micro-rotation and Re is the Reynolds number. L, u_c and T_r are the reference length, reference velocity and reference temperature respectively.

$S_w(\bar{x})$ is the dimensionless wall temperature. To facilitate a numerical solution, the equations (1-5) are transformed from the $(\bar{x}, \bar{y})$ co-ordinates to (ξ, η) new co-ordinates and the dependent variables defined as:

$$\xi=\bar{x}, \eta=\bar{y}/(\bar{x})^{1/4}, f(\xi,\eta)=\bar{\psi}/(\bar{x})^{3/4}S_w^{1/4}$$
$$N=(\bar{x})^{1/4}S_w^{3/4}g, \phi(\xi,\eta)=\theta$$
$$p(\xi)=\frac{\xi}{S_w(\xi)}\frac{dS_w(\xi)}{d\xi}, A(\xi)=\sqrt{\xi/S_w(\xi)} \quad (7)$$

The stream function is defined by:

$$\bar{u} = \frac{\partial \psi}{\partial \bar{y}} \text{ and } \bar{\upsilon} = -\frac{\partial \psi}{\partial \bar{x}}.$$

Substituting the relations (7) into the basic equations (1-5), we obtain the following system of transformed equations:

$$(1+\Delta)f''' + \left[\frac{3+p(\xi)}{4}\right]ff'' - \left[\frac{1+p(\xi)}{2}\right]f'^2 + \phi + \Delta g' = \xi(f'\frac{\partial f'}{\partial \xi} - f''\frac{\partial f}{\partial \xi}) \quad (8)$$

$$\lambda g'' + \left[\frac{3+p(\xi)}{4}\right]fg' - \left[\frac{1+3p(\xi)}{4}\right]f'g + B\Delta A(\xi)[2g + f''] = \xi(f'\frac{\partial g}{\partial \xi} - g'\frac{\partial f}{\partial \xi}) \quad (9)$$

$$\frac{1}{Pr}\phi'' + \left[\frac{3+p(\xi)}{4}\right]f\phi' - p(\xi)f'\phi' = \xi(f'\frac{\partial \phi}{\partial \xi} - \phi'\frac{\partial f}{\partial \xi}) \quad (10)$$

The transformed boundary conditions are given by

$$\eta = 0, f(\xi,0) = 0; \frac{\partial f}{\partial \xi} + \left[\frac{3+p(\xi)}{4\xi}\right]f = 0, \phi(\xi,0) = 1, g(\xi,0) = 0$$
$$\eta \to \infty: f'(\xi,\infty) = g(\xi,\infty) = \phi(\xi,\infty) = 0 \quad (11)$$

The physical quantities of primary interest are the local skin friction coefficient C_f and the local Nusselt number Nu_x which can be written respectively as:

$$C_f = 2(1+\Delta)\bar{x}^{1/4}S_w^{3/4}f''(\xi,0) \quad (12)$$

$$Nu_x = -\bar{x}^{3/4}S_w^{1/4}\phi'(\xi,0) \quad (13)$$

Numerical scheme

The numerical scheme to solve equations (8-10) adopted here is based on a combination of the following concepts:

(1) The boundary conditions for $\eta = \infty$ are replaced by

$$f'(\xi,\eta_{max}) = 0, g(\xi,\eta_{max}) = 0, \theta(\xi,\eta_{max}) = 0 \tag{14}$$

where η_{max} is a sufficiently large value of η at which the boundary conditions (14) are satisfied. In the present work, a value of $\eta_{max} = 25$ was checked to be sufficient for free stream behavior.

(2) The two-dimensional domain of interest (ξ, η) is discretized with an equispaced mesh in the ξ-direction and another equispaced mesh in the η-direction.

(3) The partial derivatives with respect to η are evaluated by the second order difference approximation.

(4) Two iteration loops based on the successive substitution are used because of the nonlinearity of the equations.

(5) In each inner iteration loop, the value of ξ is fixed while each of the equations(8-10) is solved as a linear second order boundary value problem of ODE on the η-domain. The inner iteration is continued until the nonlinear solution converges with a convergence criterion of 10^{-6} in all cases for the fixed value of ξ.

(6) In the outer iteration loop, the value of ξ is advanced from 0 to 1. The derivatives with respect to ξ are updated after every outer iteration step.

In the inner iteration step, the finite difference approximation for equations (8-10) is solved as a boundary value problem.

We consider equation (8) first. By defining $\chi = f'$ equation (8) may be written in the form

$$a_1\chi'' + b_1\chi' + c_1\chi = S_1 \tag{15}$$

where

$$\begin{aligned} a_1 &= (1+\Delta) \\ b_1 &= \left[\frac{3+p(\xi)}{4}\right]f \\ c_1 &= \left[\frac{1+p(\xi)}{2}\right]\chi \\ S_1 &= -\phi - \Delta g' + \xi\left[\chi\frac{\partial\chi}{\partial\xi} - \chi'\frac{\partial f}{\partial\xi}\right] \end{aligned} \tag{16}$$

The coefficients a_1, b_1, c_1 and the source term in equation (15) in the inner iteration step are evaluated by using the solution from the previous iteration step. Equation (15) is then transformed to a finite difference equation by applying the central difference approximations to the first and second derivatives. The finite difference equations form a tridiagonal system and can be solved by the tridiagonal solution scheme.

The gradients $\frac{\partial \chi}{\partial \xi}$ and $\frac{\partial f}{\partial \xi}$ were evaluated to a first-order finite difference approximation using the present value of ξ (unknown) and the previous value of $\xi - \Delta\xi$ (known), with the unknown present value moved to the left hand side of equation (15).

Equations (9) and (10) are also written as second-order boundary value problems similar to equation (16).

The numerical results are affected by the number of mesh points in both directions. To obtain accurate results, a mesh sensitivity study was performed. After some trials, in the η-direction 190 mesh points were chosen whereas in the ξ-direction, 11 mesh points were used. The tolerance for convergence was 10^{-6}. Increasing the mesh points to a larger value led to identical results. More details of the numerical method may be obtained from reference[9].

Results and discussion

Numerical results for the missing wall values of the velocity, microrotation and temperature fields are shown in Tables I-IV for the following cases:

case I: $$S_w = 1 - \frac{\xi}{2}$$

case II: $$S_w = 1 + \frac{\xi}{2}$$

case III: $$S_w = 1 - \frac{\xi}{2} + \frac{\xi^2}{4}$$

The results documented in Tables I-IV indicate that as Δ increases, the wall shear stress decreases, the wall couple stress decreases and the wall heat transfer rate (Nusselt number) decreases. Therefore, micropolar fluids display drag reduction and heat transfer suppression characteristics.

Figure 1 describes the details of the velocity field for case I. As Δ increases, we notice that the amplitude of the streamwise velocity decreases and the location of the maximum velocity within the boundary layer moves away from the flat surface.

From Figure 2, we observe that the wall values of the microrotation component decrease as the value of Δ increases. The microrotation component approaches monotonically zero at the boundary layer edge.

Figure 3 shows the temperature distribution within the boundary layer for the non-isothermal wall case I. Similar qualitative observations have been made for cases II and III.

ξ	S_w	Pr = 0.7 $f''(0)$	Pr = 0.7 $-\phi'(0)$	Pr = 10 $f''(0)$	Pr = 10 $-\phi'(0)$
	I	0.75814	0.53465	0.43796	1.15571
0.2	II	0.73317	0.59195	0.42280	1.2705
	III	0.7595	0.53545	0.43891	1.1568
	I	0.75395	0.52982	0.43499	1.14785
0.4	II	0.71169	0.63311	0.40960	1.3536
	III	0.76718	0.52203	0.44373	1.12937
	I	0.73557	0.54587	0.42326	1.18283
0.6	II	0.68841	0.67664	0.39539	1.44160
	III	0.78102	0.50591	0.45276	1.09477
	I	0.70415	0.5817	0.40388	1.25778
0.8	II	0.6651	0.72025	0.38128	1.52966
	III	0.80904	0.47665	0.47167	1.02957
	I	0.66263	0.63395	0.37902	1.36589
1.0	II	0.6427	0.76282	0.36783	1.6156
	III	0.86105	0.42199	0.50882	0.90035

Table I. Values for $f''(\xi, 0)$ and $\phi'(\xi, 0)$ for various values of $S_w(x)$, ξ and Pr in Newtonian fluids ($\Delta = 0$)

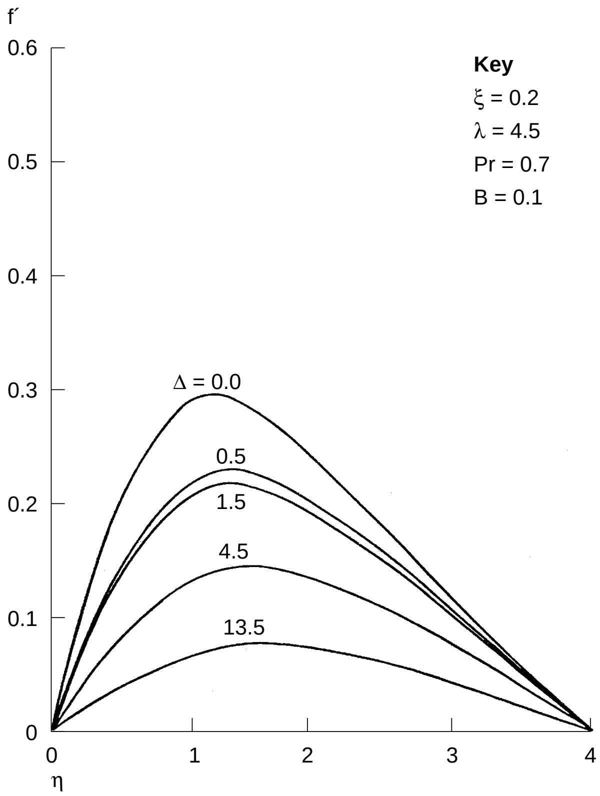

Figure 1. Velocity distribution (case I)

ξ	S_w	Pr = 0.7				Pr = 10			
		λ = 1.5							
		Δ = 0.5	Δ = 1.5	Δ = 4.5	Δ = 13.5	Δ = 0.5	Δ = 1.5	Δ = 4.5	Δ = 13.5
	I	0.56557	0.38312	0.19973	0.08398	0.32381	0.2202	0.11931	0.05457
0.2	II	0.54708	0.37109	0.19423	0.08217	0.31258	0.21264	0.1154	0.0529
	III	0.5665	0.38363	0.19986	0.08395	0.3245	0.22067	0.11956	0.05468
	I	0.56262	0.38065	0.19818	0.08367	0.32168	0.21849	0.11782	0.05368
0.4	II	0.53130	0.36035	0.18876	0.08037	0.30288	0.20592	0.11143	0.05095
	III	0.57203	0.38628	0.20022	0.08396	0.32809	0.2228	0.12011	0.05468
	I	0.54932	0.37168	0.19404	0.0827	0.31307	0.21245	0.11425	0.05199
0.6	II	0.51422	0.34897	0.18324	0.07857	0.29242	0.19875	0.10741	0.04909
	III	0.58184	0.39157	0.2018	0.08422	0.33474	0.227	0.12193	0.05537
	I	0.52644	0.35659	0.1871	0.08196	0.29882	0.20265	0.10881	0.05024
0.8	II	0.49711	0.33767	0.17781	0.07677	0.28203	0.19166	0.10354	0.04732
	III	0.60173	0.40296	0.20567	0.08485	0.34864	0.2361	0.12641	0.05725
	I	0.49609	0.33657	0.17764	0.07964	0.28053	0.19020	0.10205	0.04925
1.0	II	0.48066	0.32682	0.17259	0.07435	0.27212	0.18493	0.09989	0.04567
	III	0.6388	0.42438	0.21268	0.08503	0.37602	0.25430	0.13574	0.05925
		λ = 4.5							
	I	0.56545	0.38389	0.20167	0.08501	0.32364	0.22028	0.12045	0.05594
0.2	II	0.54695	0.37168	0.19598	0.08324	0.31242	0.21266	0.11637	0.05417
	III	0.56638	0.38439	0.20176	0.08497	0.32433	0.22074	0.12069	0.05605
	I	0.56268	0.38231	0.20094	0.08485	0.32154	0.21889	0.11943	0.05517
0.4	II	0.53126	0.36147	0.19109	0.08162	0.30273	0.20612	0.11268	0.05229
	III	0.57204	0.38784	0.20279	0.08506	0.32793	0.22319	0.12171	0.05618
	I	0.54956	0.37409	0.19738	0.08401	0.31298	0.21310	0.11609	0.05350
0.6	II	0.51425	0.35041	0.18588	0.07993	0.29229	0.19905	0.10877	0.05042
	III	0.582	0.39371	0.20462	0.08529	0.33462	0.22765	0.12385	0.05692
	I	0.52689	0.35959	0.19085	0.08227	0.29878	0.20349	0.11076	0.05098
0.8	II	0.49721	0.33931	0.18064	0.0782	0.28192	0.19203	0.10493	0.04863
	III	0.60203	0.40546	0.20841	0.08581	0.34854	0.23698	0.12858	0.05886
	I	0.49674	0.34002	0.18169	0.0795	0.28055	0.19115	0.10400	0.04786
1.0	II	0.4808	0.32859	0.17554	0.07649	0.27202	0.18534	0.10128	0.04695
	III	0.63918	0.42685	0.21486	0.08658	0.37593	0.25538	0.13816	0.06294

Table II.
Values for $f''(\xi, 0)$ for various of Δ, λ, $S_w(x)$ and Pr with B = 0.1

As Δ increases, we observe that the temperature within the boundary layer increases and approaches a linear shape for high values of Δ.

The constant Δ is proportional to spin gradient viscosity of the fluid microstructure. Increasing it results in flow retardation, which in turn decreases the rate of heat transfer convected away from the heated wall. This is clearly seen in the Figures presented.

It is observed that increasing the Prandtl number decreases the rates of microrotation. The microrotation follows fluid velocity closely as the Prantl number decreases.

Table III. Values for g′ (ξ , 0) for various of Δ, λ, S_w(x) and Pr with B = 0.1

		λ = 1.5							
		Pr = 0.7				Pr = 10			
ξ	S_w	Δ = 0.5	Δ = 1.5	Δ = 4.5	Δ = 13.5	Δ = 0.5	Δ = 1.5	Δ = 4.5	Δ = 13.5
	I	0.02902	0.06751	0.10691	0.11216	0.01049	0.02604	0.04761	0.06157
0.2	II	0.02504	0.05864	0.09461	0.10161	0.00897	0.02238	0.04155	0.05475
	III	0.02897	0.06734	0.10655	0.1117	0.01048	0.02601	0.04756	0.0615
	I	0.04347	0.09792	0.14682	0.14729	0.01597	0.03857	0.06656	0.08118
0.4	II	0.03276	0.07521	0.11703	0.12213	0.01185	0.02906	0.0518	0.06544
	III	0.04377	0.0982	0.14626	0.1456	0.01616	0.039	0.06724	0.08188
	I	0.05477	0.12053	0.17545	0.1732	0.02026	0.04784	0.07963	0.09414
0.6	II	0.03682	0.08357	0.12803	0.13257	0.01334	0.03238	0.05656	0.07016
	III	0.05715	0.12426	0.17723	0.17044	0.02147	0.05053	0.08375	0.0983
	I	0.06349	0.13741	0.19676	0.19654	0.02354	0.05458	0.08864	0.11684
0.8	II	0.03893	0.08781	0.13361	0.13831	0.0141	0.03398	0.0587	0.07216
	III	0.07129	0.15025	0.20567	0.19106	0.02736	0.06292	0.10097	0.11504
	I	0.06998	0.14968	0.21246	0.21984	0.02597	0.05933	0.09471	0.13562
1.0	II	0.03988	0.08967	0.13615	0.14021	0.01442	0.03461	0.05940	0.07270
	III	0.08832	0.17998	0.23472	0.2105	0.03500	0.07879	0.12282	0.13721
		λ = 4.5							
	I	0.00951	0.02616	0.05135	0.06669	0.00325	0.00821	0.01687	0.02598
0.2	II	0.00816	0.01976	0.0355	0.04408	0.00278	0.00702	0.01452	0.02276
	III	0.00946	0.02285	0.0405	0.04907	0.00325	0.0082	0.01685	0.02594
	I	0.01454	0.03902	0.07212	0.08828	0.00491	0.01246	0.02482	0.03596
0.4	II	0.01065	0.02579	0.04561	0.05509	0.00365	0.00925	0.01877	0.0282
	III	0.01431	0.03428	0.05855	0.06709	0.00498	0.0126	0.02506	0.03625
	I	0.01852	0.04867	0.08658	0.10283	0.00622	0.01579	0.03068	0.04282
0.6	II	0.01198	0.02897	0.05094	0.06096	0.00409	0.0104	0.02088	0.03073
	III	0.01878	0.04441	0.07327	0.08055	0.00662	0.01669	0.03227	0.04477
	I	0.02159	0.05574	0.09665	0.1129	0.00723	0.01834	0.03497	0.04758
0.8	II	0.01263	0.03066	0.05386	0.06435	0.00431	0.01098	0.02191	0.03188
	III	0.02362	0.05481	0.08695	0.09172	0.00848	0.02119	0.03993	0.0535
	I	0.02379	0.06068	0.10347	0.11978	0.00799	0.02026	0.03803	0.05083
1.0	II	0.01292	0.03147	0.05536	0.06627	0.00441	0.01123	0.0223	0.03228
	III	0.02955	0.06682	0.10072	0.10119	0.01092	0.02702	0.04966	0.06439

A comparison will be made between the Newtonian fluid values and micropolar fluid values for friction factor and heat transfer rates (in dimensionless form, Nusselt number). For this purpose, we make reference to Tables I, II and IV. Considering case I, the solution corresponding to ξ = 0.2 and Pr = 0.7 indicates that $f''(\xi, 0)$ for Newtonian fluids is 0.75814 whereas for micropolar fluids (Δ = 4.5 and λ = 1.5) it is 0.19973.

Similarly, the heat transfer rates are proportional to 0.53465 and 0.37129 for Newtonian fluids and micropolar fluids, respectively. This indicates that micropolar fluids display drag reduction and heat transfer rate reduction properties.

ξ	S_w	Pr = 0.7				Pr = 10			
		$\Delta = 0.5$	$\Delta = 1.5$	$\Delta = 4.5$	$\Delta = 13.5$	$\Delta = 0.5$	$\Delta = 1.5$	$\Delta = 4.5$	$\Delta = 13.5$
					$\lambda = 1.5$				
	I	0.4906	0.43851	0.37129	0.31344	1.04654	0.92377	0.76452	0.61099
0.2	II	0.54238	0.48348	0.40629	0.33768	1.15024	1.01475	0.83841	0.66849
	III	0.49132	0.43916	0.372	0.31435	1.04753	0.92459	0.76509	0.61131
	I	0.4867	0.43632	0.3708	0.31167	1.04015	0.91984	0.76492	0.61452
0.4	II	0.57999	0.51741	0.43468	0.35767	1.22593	1.08258	0.89666	0.71725
	III	0.47955	0.43016	0.36696	0.31148	1.02321	0.90461	0.75182	0.6034
	I	0.50184	0.45056	0.38258	0.3173	1.0725	0.9498	0.79248	0.63877
0.6	II	0.61979	0.55306	0.46414	0.37863	1.30587	1.15376	0.9567	0.76642
	III	0.46524	0.4187	0.35985	0.30832	0.99218	0.87817	0.73185	0.58847
	I	0.56421	0.48114	0.40793	0.19654	1.14112	1.01172	0.84623	0.64788
0.8	II	0.65973	0.58883	0.49379	0.40021	1.38588	1.22481	1.01621	0.81483
	III	0.43911	0.39721	0.34613	0.30322	0.93324	0.82665	0.6901	0.5508
	I	0.58391	0.52598	0.44617	0.15468	1.23993	1.10033	0.92206	0.6574
1.0	II	0.69877	0.62386	0.52301	0.4325	1.46395	1.29405	1.074	0.86167
	III	0.39056	0.35785	0.32284	0.30146	0.81605	0.72301	0.6037	0.53461
					$\lambda = 4.5$				
	I	0.49939	0.449081	0.37531	0.30342	1.07304	0.91998	0.7544	0.59395
0.2	II	0.54176	0.48064	0.39908	0.32966	1.09999	1.01113	0.82874	0.6514
	III	0.49069	0.43628	0.36511	0.30766	1.07334	0.92082	0.75503	0.59434
	I	0.49549	0.44653	0.37731	0.305	1.03886	0.91508	0.75272	0.59628
0.4	II	0.57918	0.51384	0.42602	0.34839	1.22476	1.07827	0.88548	0.69863
	III	0.47871	0.42657	0.35933	0.30518	1.02195	0.89996	0.73996	0.58568
	I	0.51076	0.46097	0.39108	0.317	1.07097	0.94429	0.77871	0.61957
0.6	II	0.61885	0.54902	0.45444	0.3682	1.30456	1.14905	0.94465	0.74677
	III	0.46427	0.41479	0.35236	0.30277	0.99075	0.87298	0.71911	0.57098
	I	0.54393	0.49141	0.41822	0.2989	1.13938	1.00555	0.83103	0.66352
0.8	II	0.65869	0.58446	0.48328	0.3887	1.38447	1.21985	1.00359	0.79431
	III	0.4381	0.39346	0.3398	0.33989	0.93172	0.82124	0.67734	0.53876
	I	0.59175	0.53505	0.4566	0.37236	1.23801	1.09358	0.90550	0.72508
1.0	II	0.69766	0.61924	0.51185	0.40949	1.46246	1.28893	1.06096	0.84039
	III	0.3897	0.3552	0.31943	0.29404	0.81465	0.71813	0.59266	0.47165

Table IV.
Values of $\phi'(\xi, 0)$ for various of Δ, λ, $S_w(x)$ and Pr with B = 0.1

A comment will be made on the boundary condition of microrotation at the wall as given by equation (5). We considered $\underline{\bar{N}} = -n_1 (\partial \bar{u} / \partial \bar{y})$ where $n_1 = 0$ has been used in this paper . This case corresponding to n = ½ results in the vanishing of the antisymmetric part of the stress tensor and is believed to represent weak concentrations. The case corresponding to $n_1 = 1$ is applicable to the modeling

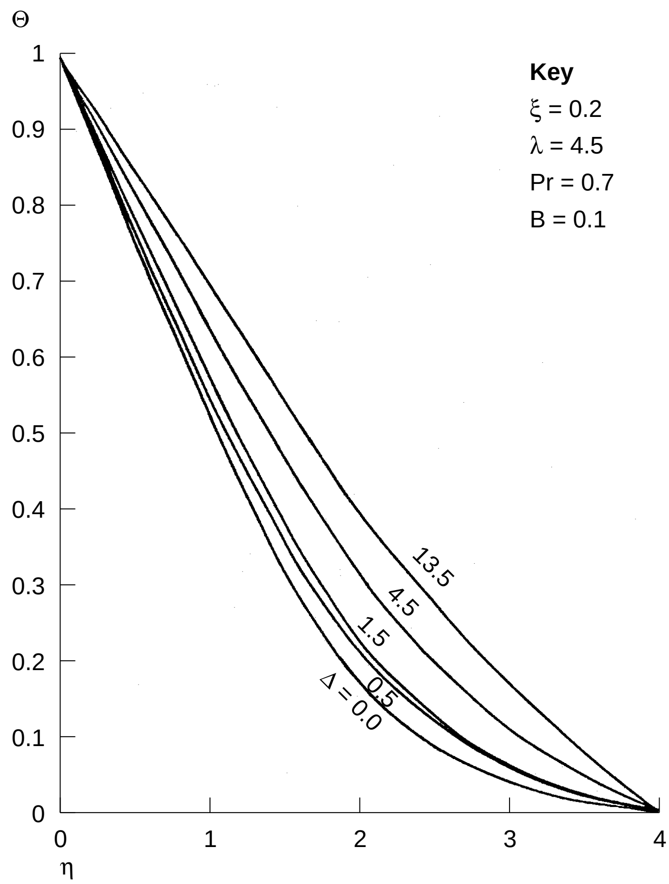

Figure 2. Microrotation distribution (case I)

of turbulent flows. For $n_1 = 0$ (high concentration), particles are not free to rotate and hence the values of $\bar{N}$ are small.

As n_1 increases to 0.5 and 1.0 from zero, the microrotation also increases accordingly, resulting in considerable flow enhancement.

Concluding remarks

The problem of the nonsimilar free convection boundary layer flow of a micropolar fluid has been considered in this paper. Three different thermal boundary conditions are considered. The transformed governing equations are solved numerically by means of a finite difference method and results are presented for the velocity, angular velocity and temperature fields. The numerical results indicate that the micropolar fluids display drag and heat transfer rate reduction properties.

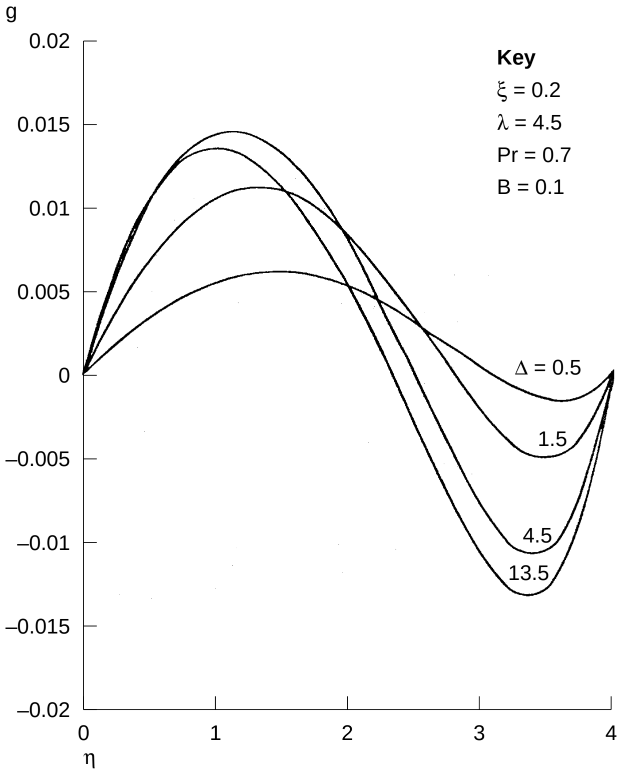

Figure 3.
Temperature distribution (case I)

References

1. Eringen, A.C., "Theory of micropolar fluids", *Journal of Mathematics and Mechanics*, Vol. 6, 1996, pp. 1-18.
2. Eringen, A.C., "Theory of thermomicrofluids", *Mathematical Analysis and Applications*, Vol. 38, 1972, pp. 480-96.
3. Ahmadi, G., "Self-similar solution of incompressible micropolar boundary layer flow over semi-infinite plate", *International Journal of Engineering Science*, Vol. 14, 1976, pp. 639 -46.
4. Gorla, R.S.R., "Heat transfer in micropolar boundary layer flow over a flat plate", *International Journal of Engineering Science*, Vol. 21, 1983, pp. 791-8.
5. Jena, S.K. and Mathur, M.M., "Similarity solution for laminar free convective flow of thermomicropolar fluid past a non-isothermal vertical plate", *International Journal of Engineering Science*, Vol. 19, 1981, pp. 1431-39.
6. Gorla, R.S.R., Ling, P. and Yang, A., "Asymptotic boundary layer solution for mixed convection from a vertical surface in a micropolar fluid", *International Journal of Engineering Science*, Vol. 28, 1990, pp. 525-33.
7. Gorla, R.S.R., "Mixed convection in a micropolar fluid from a vertical surface with uniform heat flux", *International Journal of Engineering Science*, Vol. 30, 1992, pp. 349-58.
8. Gorla, R.S.R., "Mixed convection boundary layer flow of a micropolar fluid on a horizontal plate", *Acta Mechanical Journal*, Vol. 108, 1995, pp. 101-10.
9. Gorla, R.S.R., Lee, J.K., Nakamura, S. and Pop, I., "Effects of transverse magnetic field on mixed convection in wall plume of power-law fluids", *International Journal of Engineering Science*, Vol. 31, 1993, pp. 1035-45.